tvst

Retina

SZN-413, a FZD4 Agonist, as a Potential Novel Therapeutic for the Treatment of Diabetic Retinopathy

Huy Nguyen[1], Hui Chen[1], Meghah Vuppalapaty[1], Elizabeth Whisler[1], Kelsey Ronarda Logas[1], Parthasarathy Sampathkumar[1], Russell Byron Fletcher[1], Asmiti Sura[1], Nicholas Suen[1], Suhani Gupta[1], Tom Lopez[1], Jay Ye[1], Shengjiang Tu[1], Menaka Bolaki[1], Wen-Chen Yeh[1], Yang Li[1], and Sung-Jin Lee[1]

[1] Surrozen Operating, Inc., South San Francisco, CA, USA

Correspondence: Sung-Jin Lee, Surrozen Operating, Inc., 171 Oyster Point Boulevard, Suite 400, South San Francisco, CA 94080, USA.
e-mail: sungjin@surrozen.com
Yang Li, Surrozen Operating, Inc., 171 Oyster Point Boulevard, Suite 400, South San Francisco, CA 94080, USA.
e-mail: yang@surrozen.com

Received: May 10, 2022
Accepted: August 15, 2022
Published: September 23, 2022

Keywords: Wnt; FZD4; FZD4-specific agonist; endothelial cells; diabetic retinopathy

Citation: Nguyen H, Chen H, Vuppalapaty M, Whisler E, Logas KR, Sampathkumar P, Fletcher RB, Sura A, Suen N, Gupta S, Lopez T, Ye J, Tu S, Bolaki M, Yeh WC, Li Y, Lee SJ. SZN-413, a FZD4 agonist, as a potential novel therapeutic for the treatment of diabetic retinopathy. Transl Vis Sci Technol. 2022;11(9):19, https://doi.org/10.1167/tvst.11.9.19

Purpose: There remains a high unmet need for therapies with new mechanisms of action to achieve reperfusion of ischemic retina in diabetic retinopathy. We examined whether a novel frizzled class receptor 4 (FZD4) agonist could promote regeneration of functional blood vessels in animal models of retinopathy.

Methods: We developed a novel Norrin mimetic (SZN-413-p) targeting FZD4 and low-density lipoprotein receptor-related protein 5 (LRP5) and examined its effect on retinal and brain endothelial cells in vitro. SZN-413-p was subsequently humanized, resulting in the therapeutic candidate SZN-413, and was examined in animal models of retinopathy. In an oxygen-induced retinopathy mouse model, avascular and neovascularization areas were measured. Furthermore, in a vascular endothelial growth factor (VEGF)-induced retinal vascular leakage rabbit model, the impact on vascular leakage by SZN-413 was examined by measuring fluorescein leakage.

Results: SZN-413-p induced Wnt/β-catenin signaling and upregulated blood–brain barrier/blood–retina barrier gene expressions in endothelial cells. In the oxygen-induced retinopathy mouse model, SZN-413-p and SZN-413 significantly reduced the neovascularization area size ($P < 0.001$) to a level comparable to, or better than the positive control aflibercept. Both agonists also showed a reduction in avascular area size compared to vehicle ($P < 0.001$) and aflibercept groups ($P < 0.05$ and $P < 0.01$ for SZN-413-p and SZN-413, respectively). In the VEGF-induced retinal vascular leakage rabbit model, SZN-413 reduced retinal vascular leakage by ~80%, compared to the vehicle-treated group ($P < 0.01$).

Conclusions: Reduction of neovascular tufts and avascular areas and of VEGF-driven retinal vascular leakage suggests that SZN-413 can simultaneously address retinal non-perfusion and vascular leakage.

Translational Relevance: FZD4 signaling modulation by SZN-413 is a novel mechanism of action that can offer a new therapeutic strategy for diabetic retinopathy.

Introduction

Diabetic retinopathy (DR), a specific microvascular complication of diabetes, is a major cause of vision loss in the middle-aged, economically active demographic.[1–3] The increasing number of diabetic retinopathy patients is currently recognized as a serious public health problem. In fact, studies have shown that, although all causes of blindness and visual impairment (all ages) declined significantly between 1990 and 2015, diabetic retinopathy increased steadily.[4]

DR may progress to diabetic macular edema (DME) and proliferative DR, causing loss of vision.[5] The pathogenesis of DR, including DME, is characterized by pericyte loss, thickening of endothelial cell basement membranes, and development of microaneurysms contributing to the disruption and

breakdown of the blood–retina barrier (BRB). This loss of normal retinal vasculature and areas of retinal non-perfusion, a key pathologic feature of DR, can lead to tissue ischemia of the metabolically active retina, resulting in hypoxia and the overproduction of multiple signaling molecules, such as hypoxia-inducible factor 1-alpha, vascular endothelial growth factor A (VEGF-A), angiopoietin-2, tissue inhibitor matrix metalloproteinase 1, and angiopoietin-like 4.[6] These factors will in turn contribute to vascular leakage, increased vessel permeability, and pathologic angiogenesis in the oxygen-deprived retina.

VEGF is an important factor in the development of wet-type age-related macular degeneration (wAMD), proliferative DR, and DME,[7,8] inducing pathologic neovascularization and altering retinal capillary permeability.[9] Anti-VEGF agents, such as aflibercept and ranibizumab, control ocular neovascularization, leakage, and intraocular inflammation[10] and are currently the standard of care in the treatment of DME and wAMD. These agents have also been shown to improve DR severity score (DRSS) levels in eyes both with and without DME and to reduce the progression of non-proliferative DR to proliferative DR.[11–14] Multiple prospective datasets have reported that retinal non-perfusion may continue to accumulate despite regular anti-VEGF dosing in many DR patients and that anti-VEGF therapy does not induce reperfusion of ischemic retinal areas.[5] Therefore, there remains a high unmet need for therapies with new mechanisms of action to achieve clinically meaningful retinal reperfusion of ischemic areas in DR, reduce retinal ischemia, and reduce the ensuing production of factors contributing to vascular leakage and pathologic angiogenesis. Furthermore, although anti-VEGF therapy is effective in treating DME and DR, frequent dosing is required, and there is still a need for agents with a longer treatment effect.

Frizzled class receptor 4 (FZD4)-specific Wnt/β-catenin signaling plays a critical role in proper vascular development and barrier function in the central nervous system and the retina and in the maintenance of the integrity of the adult blood–brain barrier (BBB) and BRB.[15–18] Growing genetic evidence from human and rodent studies further supports the importance of FZD4-dependent Wnt/β-catenin signaling in retinal vasculature. Human mutations in genes encoding either receptors (*FZD4*, *LRP5*, and *TSPAN12*) or the ligand Norrin (*NDP*), involved in Wnt/β-catenin signaling, result in a variety of inherited vitreoretinopathies.[19–21] Mutations of these genes in mice also show the typical aberrant vasculature seen in human retinopathy.[15,18,21,22]

Activation of FZD4 signaling induces protein expressions for vascular barrier functions (e.g., claudin-5 [Cldn5], zonula occludens-1 [Zo-1], major facilitator superfamily domain containing 2 [Mfsd2]) and reduces the expression of plasmalemma vesicle-associated protein (Plvap), a marker of immature or leaky retinal vessels,[23–25] which restrains vascular leakage. Additionally, it has been shown that intravitreal injection of Norrin can restore the BRB properties to some degree in streptozotocin-induced diabetic rats[26] and that stabilizing β-catenin in the choriocapillaris switches its permeable nature to a BRB-like state.[27] Taken together, these findings underscore the potential of targeting the FZD4-specific Wnt/β-catenin pathway as a new therapeutic strategy for the treatment of diabetic retinopathies.

In the current study, we generated a novel FZD4-specific agonist, SZN-413, and observed that it potently inhibited pathologic neovascularization (NV) in mouse models of oxygen-induced retinopathy (OIR). Furthermore, SZN-413 induced proper retinal vessel regrowth, suggesting the potential to re-perfuse the ischemic retina in DR. The FZD4-specific agonist also prevented the retinal leakage induced by VEGF, a prominent factor in the pathogenesis of DR. The current findings suggest that activation of FZD4 signaling may simultaneously address the retinal non-perfusion and leakage characteristics of DR pathology.

Materials and Methods

Molecular Cloning and Protein Generation

Constructs for SZN-413-p and SZN-413 were cloned into pcDNA3.1(+) mammalian expression vector (Thermo Fisher Scientific, Waltham, MA). Recombinant proteins were produced in Expi293F cells (Thermo Fisher Scientific) by transient transfection. The SZN-413-p and SZN-413 proteins were first purified with CaptivA Protein A Affinity Resin (Repligen, Waltham, MA) and further polished with Superdex 200 Increase 10/300 GL (GE Healthcare Life Sciences, Piscataway, NJ) size-exclusion chromatography (SEC) using 1× HEPES buffered saline (20-mM HEPES, pH 7.4; 150-mM NaCl) or 2× HEPES buffered saline (40-mM HEPES, pH 7.4; 300-mM NaCl). The cysteine-rich domains (CRDs) of 10 FZDs were expressed and purified as previously described.[28] All proteins were also examined by sodium dodecyl

sulfate–polyacrylamide electrophoresis and estimated to be >90% pure.

Affinity Measurement and Binding Specificity

Binding kinetics and specificity of anti-FZD4 immunoglobulin G (IgG), anti-FZD4 Fab, SZN-413-p, and SZN-413 to human FZD CRDs were determined by biolayer interferometry using an Octet Red 96 instrument (Pall ForteBio, Fremont, CA) at 30°C and 1000 rpm with streptavidin (SA) biosensors. Biotinylated FZD4 CRD was diluted to 50 nM in the running buffer (phosphate-buffered saline, 0.05% Tween-20, 0.5% bovine serum albumin, pH 7.2) and captured by the SA biosensor (Sartorius, Göttingen, Germany), followed by dipping into wells containing the anti-FZD4 IgG, anti-FZD4 Fab, or SZN-413-p at different concentrations in a running buffer or into a well with only the running buffer as a reference channel. SZN-413 or mouse Fzd4-Fc (R&D Systems, Minneapolis, MN) were diluted to 50 nM in the running buffer and captured by an anti-human IgG capture (AHC) biosensor (Sartorius), followed by dipping into wells containing the FZD4 CRD or anti-FZD4 Fab at different concentrations in a running buffer or into a well with only the running buffer as reference channel. The dissociation of the interaction was followed with the running buffer. The monovalent K_D for each binder was calculated using the Octet system software, based on fitting to a 1:1 binding model. For the binding specificity test, 10 human FZD CRDs were diluted to 50 nM in the running buffer and captured by the SA biosensor, followed by dipping into wells containing anti-FZD4 IgG and SZN-413-p. SZN-413 was diluted to 50 nM in the running buffer and captured by the AHC biosensor, followed by dipping into wells containing the 10 human FZD CRDs in the running buffer.

SuperTop Flash Assay

Wnt/β-catenin signaling activity was measured using human embryonic kidney endothelial cell line 293 (HEK293), human retinal microvascular endothelial cells (HRMECs), mouse brain microvascular endothelial cells (bEnd.3), and rabbit retinal microvascular endothelial cells. In brief, Wnt/β-catenin signaling activity was measured using HEK293 cells containing a luciferase gene controlled by a Wnt-responsive promoter (Super Top Flash reporter assay [STF]), as previously reported.[29] The bEnd.3 cells were stably transfected with the STF plasmid and a constitutively expressed renilla luciferase. HRMECs and rabbit retinal microvascular endothelial cells were transiently transfected with the STF plasmid for the STF assay. Cells were seeded at a density of 10,000 cells per well in 96-well plates 24 hours prior to treatment in the presence of 3-μM inhibitor of Wnt production 2 (IWP2) to inhibit the production of endogenous Wnts. SZN-413-p or SZN-413 proteins were then added to the cells for 16 to 18 hours. Recombinant human WNT3A (R&D Systems) and the recombinant human Norrin (R&D Systems) were used as response comparators. Cells were lysed with Luciferase Cell Culture Lysis Reagent (Promega, Madison, WI), and luciferase activity was measured with the Promega Luciferase Assay System using vendor-suggested procedures.

Western Blot Analysis

Western blot analysis was performed as previously reported,[30] with minor modifications. In brief, HRMECs were treated with 10-nM SZN-413-p 24 hours before harvesting for cell lysis. The anti-ZO-1 (ab216880; Abcam, Cambridge, UK), anti-CLDN5 (ab131259; Abcam), and anti-β actin (A5441; Sigma-Aldrich, St. Louis, MO) primary antibodies were used, followed by horseradish peroxidase-conjugated anti-rabbit or anti-mouse secondary antibodies for chemiluminescent signals.

Quantitative Polymerase Chain Reaction Analysis of Gene Expression

RNAs from HRMECs, bEnd.3 cells, or human umbilical vein endothelial cells (HUVECs) were extracted using the Qiagen RNeasy Micro Kit (Qiagen, Hilden, Germany). cDNA was produced using the SuperScript IV VILO cDNA Synthesis Kit (Thermo Fisher Scientific). RNA was quantified using TaqMan Fast Advanced Master Mix (Thermo Fisher Scientific) with the following Thermo Fisher Scientific probes: Mm00445405_s1 *Fzd1*, Mm02524776_s1 *Fzd2*, Mm00445423_m1 *Fzd3*, Mm00433382_m1 *Fzd4*, Mm00445623_s1 *Fzd5*, Mm00433387_m1 *Fzd6*, Mm00433409_s1 *Fzd7*, Mm01234717_s1 *Fzd8*, Mm01206511_s1 *Fzd9*, Mm00558396_s1 *Fzd10*, Mm01227476_m1 *Lrp5*, Mm00999795_m1 *Lrp6*, Hs00268943_s1 *FZD1*, Hs00361432_s1 *FZD2*, Hs00907280_m1 *FZD3*, Hs00201853_m1 *FZD4*, Hs00258278_s1 *FZD5*, Hs01095627_m1 *FZD6*, Hs00275833_s1 *FZD7*, Hs00259040_s1 *FZD8*, Hs00268954_s1 *FZD9*, Hs00273077_s1 *FZD10*, Hs00182031_m1 *LRP5*, Hs00233945_m1 *LRP6*, Hs01547250_m1 *LEF1*, Hs00293017_m1 *MFSD2A*, Hs00610344-m1 *AXIN2*, and Mm00443610_m1

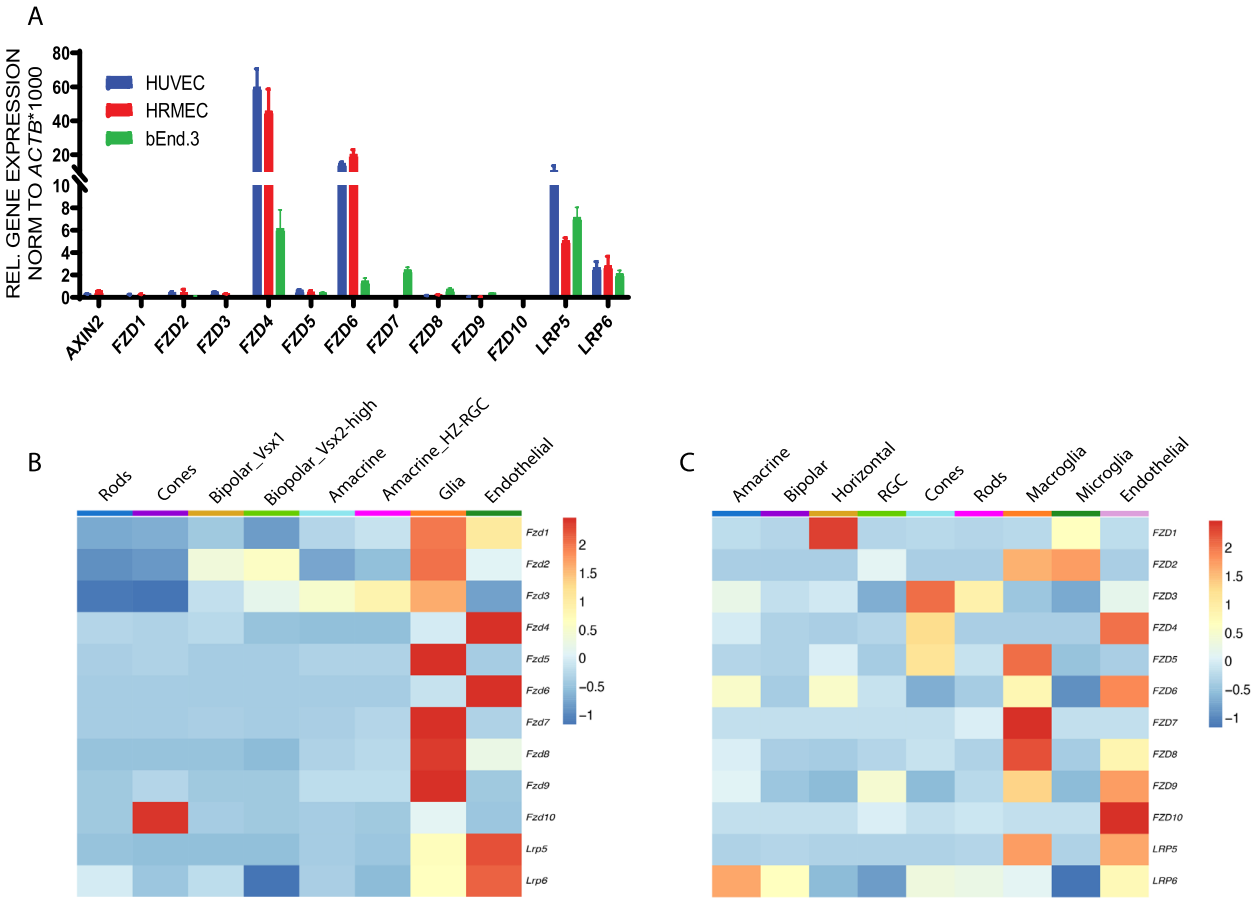

Figure 1. FZD4 and LRP5, primary receptors for Wnt signaling in vascular endothelial cells. (A) *FZD1–10* and *LRP5* and *LRP6* mRNA expression in HRMECs, bEnd.3 cells, and HUVECs quantified by quantitative polymerase chain reaction (qPCR) and normalized by the housekeeping gene *Actin*. Bars represent mean ± SD. (B) Data from Macosko et al.[31] were reanalyzed to derive scaled average gene expression by cell type of Wnt receptors in mouse retina. (C) Data from Menon et al.[34] were reanalyzed to derive scaled average gene expression by cell type of Wnt receptors in human retina.

Axin2. Cycle threshold (C_t) values were normalized to the expression of constitutive *ActinB* RNA using Mm02619580_g1 or *ACTINB* RNA using Hs01060665_g1.

Single-Cell RNA Sequencing Data Analysis

Droplet single-cell RNA sequencing (scRNA-seq) data from naïve, uninjured mice at P14[31] were reanalyzed. Briefly, the data were filtered based on cell quality metrics using SCONE 1.14.0,[32] the number of genes detected, and percentage of mitochondrial gene expression, yielding 44,489 cells. Gene expression values were normalized by deconvolution scaling using the Scran 1.18.6[33] and Scuttle 1.04 packages for R (R Foundation for Statistical Computing, Vienna, Austria). Cells were clustered into broad cell-type categories, and the average normalized expression for each cell type or group of cell types was scaled for each gene presented in the heatmap in Figure 1B. Droplet scRNA-seq data from postmortem human retinas[34] were reanalyzed. The processed counts matrix including 20,091 cells and 19,719 genes was downloaded. Gene expression values were normalized by deconvolution scaling using the Scran 1.18.6[33] and Scuttle 1.04 R packages. Cell-type annotations provided by the authors were used, and the average normalized expression for each cell type was scaled for each gene presented in the heatmap in Figure 1C.

OIR Study

A mouse model of OIR was created as previously described.[35] Briefly, newborn pups at postnatal day 7 (P7) were exposed to a hyperoxic environment with a 75% inspired oxygen level for 5 days. As a result,

the pups developed avascular (AV) retina from vaso-obliteration of newly formed capillaries in the center retina from P7 to P12. After the pups were moved to room air at P12, the AV central retina became hypoxic and intravitreal neovascular (NV) tufts formed at the junctions of the vascular and AV retina from P12 to P17. For treatment, P12 pups received an intravitreal injection of a test article (68 ng of SZN-413-p, 13.6 ng of SZN-413, or 60 µg of aflibercept) or vehicle control (see Fig. 4). In the dose–efficacy relationship study (see Fig. 5), 13.6 ng, 136 ng, and 1360 ng of SZN-413 or vehicle control were injected. To evaluate the efficacy of test articles on reducing AV and NV areas, whole-mount retinas from pups at P17 were stained with isolectin B4 and imaged. AV, NV, and total retinal areas were manually scored and presented as a percentage of either AV or NV area over total retinal area. Statistical significance between each treatment group and the vehicle control group was determined using a one-way analysis of variance (ANOVA) test followed by Tukey's multiple comparison test.

VEGF-Induced Retinal Hemorrhage Study

On day 0, Dutch Belted rabbits were dilated with 1% tropicamide hydrochloric acid (HCl), then tranquilized before being given injections of buprenorphine 0.05 mg/kg subcutaneously or meloxicam 0.1 mg/kg intramuscularly. Both eyes were aseptically prepared using topical 5% betadine solution, followed by rinsing with sterile eye wash and application of one drop of 0.5% proparacaine HCl. Immediately after injection of vehicle, SZN-413 (10 µg/eye), SZN-413 (2 µg/eye), SZN-413 (0.4 µg/eye), or SZN-413 0.08 (µg/eye), retinal vascular leakage was induced via injection of $VEGF_{165}$ (#293-VE-050/CF; R&D Systems) into the left eyes of all animals using a 30-gauge needle. The dose of the $VEGF_{165}$ injections was 1.0 µg in 50 µL balanced salt solution. Following the injection, one drop of antibiotic ophthalmic solution (neomycin, polymyxin B sulfates, and gramicidin) was applied topically to the ocular surface. Following $VEGF_{165}$ injection, the animals were returned to their cages and allowed to recover normally. Fluorescein angiography (FA) was done in the left eyes of all animals at days 0, 3, and 5 post-injection. Mydriasis for FA was done using topical 1% tropicamide HCl (one drop to both eyes 15 minutes prior to examination). Early-phase retinal photography was performed at 1 to 2 minutes after intravenous sodium fluorescein injection (12 mg/kg). Images were assessed, masked, and scored for retinal vascular leakage by two trained scorers utilizing the semiquantitative scale below:

Score	Retinal Leakage
0	Major blood vessels appear very straight with limited tortuosity of smaller vessels.
1	Major blood vessels present increased tortuosity and/or vessel dilation.
2	Leakage is present between major vessels, no leakage between minor vessels.
3	Leakage is present between major and minor vessels.
4	Leakage is present between major and minor vessels. Minor vessels are not visible.

Statistical significance between each treatment group and the vehicle control group was determined using a one-way ANOVA test followed by Dunnett's multiple comparison test.

A veterinary ophthalmologist performed complete ocular examinations using a slit-lamp biomicroscope and indirect ophthalmoscope to evaluate ocular surface morphology, anterior segment and posterior segment inflammation, cataract formation, and retinal changes on all animals prior to intravitreal injections to serve as a baseline and on days 3 and 5 following administration of the test articles and VEGF. The modified Hackett and McDonald ocular grading system[36] was used for scoring. A score of 0 indicates no inflammation, 1 to 4 is mild inflammation, 5 to 10 is moderate inflammation, and >11 is severe inflammation. Data are presented as mean ± standard deviation (SD). Animals were not tranquilized for the examinations.

Animal Study Treatments

All animal experiments were performed according to national ethical guidelines and with the guidance and approval of the Institutional Animal Care and Use Committee of Surrozen, Inc. All experiments conformed with the ARVO Statement for the Use of Animals in Ophthalmic and Vision Research.

Results

Wnt Receptor Expression Profiles from Retinal Vascular Endothelial Cells

Human and rodent genetics have identified FZD4 and low-density lipoprotein receptor-related protein 5 (LRP5) as the important Wnt receptors for retinal vascular development and its barrier function.[17,37,38] We confirmed that FZD4 and LRP5 are abundantly expressed in HRMECs, HUVECs, and bEnd.3 cells (Fig. 1A). To further understand the expression

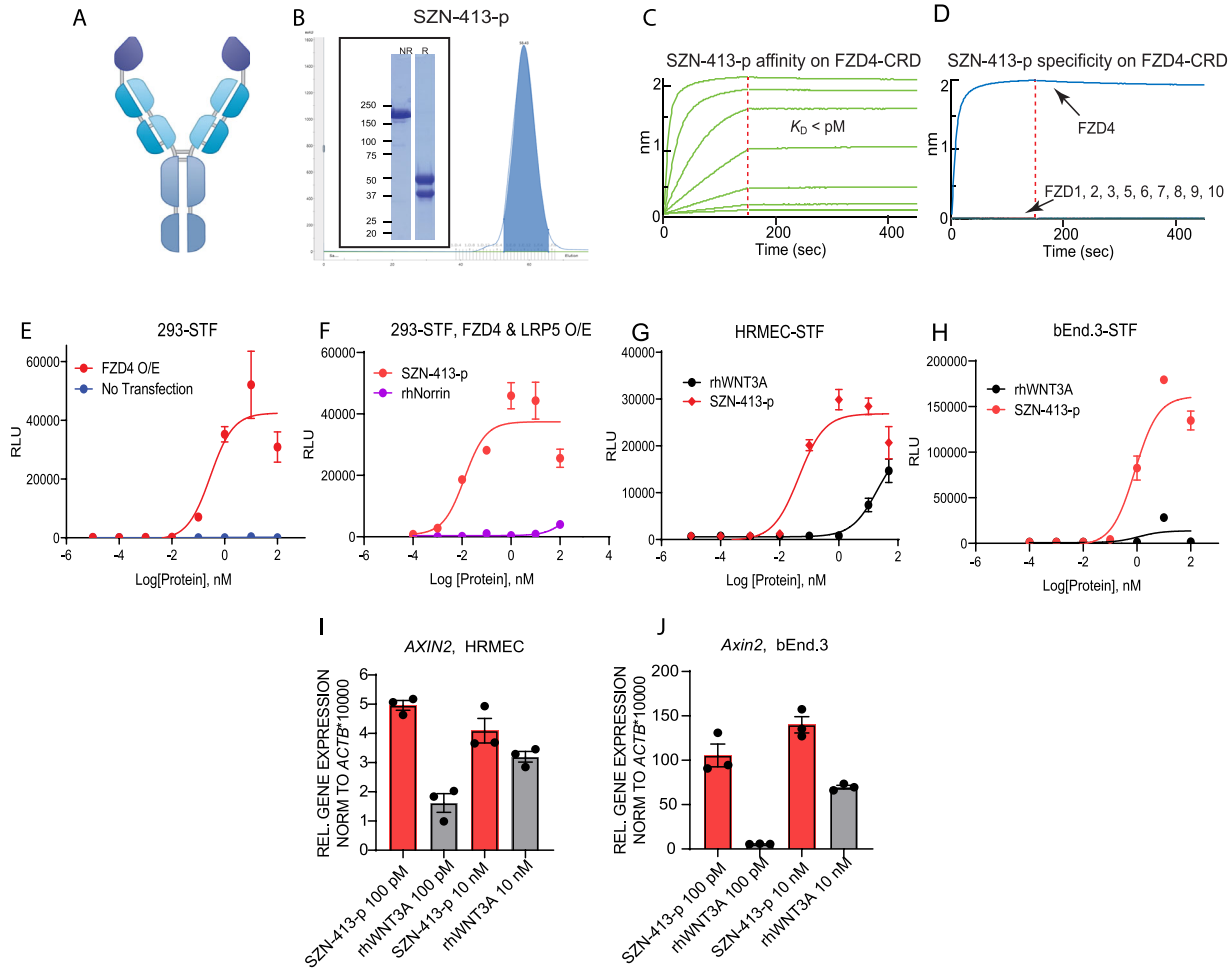

Figure 2. FZD4-specific Wnt/β-catenin signaling agonist SZN-413-p. (A) Schematic diagram of SZN-413-p. (B) SZN-413-p production and purification with SEC. SZN-413-p with high purity (*insert*) after the SEC purification. NR, non-reducing; R, reducing. (C) The binding affinity of SZN-413-p to human FZD4 CRD (bivalent) measured on the Octet. (D) Binding specificity of SZN-413-p to all 10 human FZD CRDs measured on the Octet. (E) Dose-dependent STF activity of SZN-413-p in 293STF cells or FZD4-transfected 293STF cells. (F) Dose-dependent STF activity of SZN-413-p or Norrin in 293STF cells transfected with both FZD4 and LRP5. (G, H) Dose-dependent STF activities of the SZN-413-p or WNT3A in HRMECs (G) and bEnd.3 cells (H). (I, J). Quantitative reverse transcription polymerase chain reaction (qRT-PCR) results of *Axin2* gene expressions in HRMECs (I) and bEnd.3 cells (J). The mRNA expression values were normalized by *Actin* gene expression. Graphs are shown as mean ± SD.

patterns of Wnt receptors in different cell types in the retina, we analyzed previously published scRNA-seq data on uninjured, naïve P14 mouse retinas.[31] We identified the major cell types of the mouse and human retina based on previously established markers and published annotations and then assessed the expression of Wnt signaling pathway components (Figs. 1B, 1C). This analysis confirmed that FZD4 and LRP5 are the most abundant and relatively specific receptors expressed in the endothelial cells (ECs). Therefore, targeting the FZD4/LRP5 combination not only allows induction of Wnt signaling in the ECs but also may provide more specificity for ECs.

The Bioengineered FZD4 Agonist, SZN-413-p, Is Active in Vascular Endothelial Cells

Given the evidence supporting the importance of FZD4 and LRP5 in retinal vascular biology and to more specifically induce Wnt/β-catenin signaling in ECs, we generated a FZD4/LRP5-targeting Norrin mimetic molecule to study its effects on retinal vascular EC function. A FZD4-binding IgG was identified from a phage library containing human single-chain variable fragments. The anti-FZD4 IgG showed high affinity binding to human FZD4 CRD but not to the other nine human FZD CRDs (Supplementary Fig. S1). The

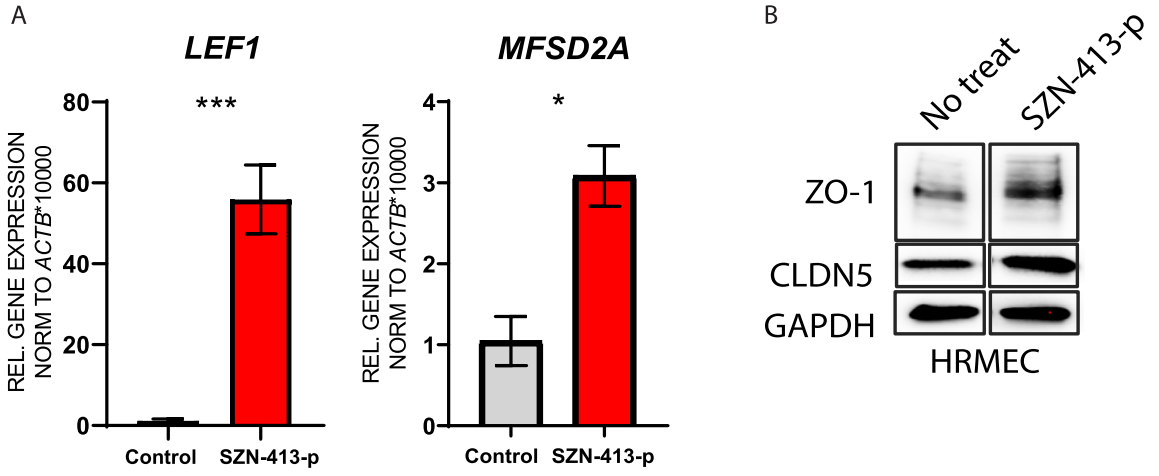

Figure 3. SZN-413-p induced BBB/BRB gene expression. (A) The qRT-PCR results for *LEF1* and *MFSD2A* gene expression in HRMECs. The mRNA expression values were normalized by *ACTIN* gene expression. (B) Upregulation of ZO-1 and CLDN5 protein expression in HRMECs after the SZN-413-p treatment. Values are mean ± SEM; ***$P < 0.001$.

FZD4 CRD sequences are highly conserved among human, mouse, and rabbit (Supplementary Fig. S2A). The anti-FZD4 Fab showed tight bindings to both human and mouse FZD4 CRDs (Supplementary Fig. S2B). The extracellular domain sequences of LRP5 are also highly conserved across species (Supplementary Fig. S2C). We selected a proprietary LRP5-biased binder[39] and fused it to the N-terminal end of the anti-FZD4 IgG light chain in the tetravalent bispecific formats, yielding the Norrin-mimetic molecule, SZN-413-p (Fig. 2A). SZN-413-p was expressed and purified to homogeneity, and its binding specificity and affinity to FZD4 were confirmed with a biolayer interferometry assay (Figs. 2B–2D). The ability of SZN-413-p to activate Wnt/β-catenin signaling was assessed in the Wnt-responsive HEK293 STF reporter cells (293STF assay).[29] Although SZN-413-p did not induce a strong response in parental 293STF cells due to low expression levels of endogenous FZD4, SZN-413-p strongly activated Wnt/β-catenin signaling in the 293STF cells transfected with FZD4 in a dose-dependent manner (Fig. 2E). The STF response with SZN-413-p was far stronger than that with the recombinant Norrin protein in the assay (Fig. 2F).

We further performed the STF reporter assay in two microvascular ECs, HRMECs (human retina) and bEnd.3 cells (mouse brain). Unlike in the 293STF cells, SZN-413-p induced dose-dependent STF responses in both vascular ECs without overexpression of FZD4, and again the response with SZN-413-p was stronger than that with the comparator, recombinant WNT3A (Figs. 2G, 2H). These results not only showed that SZN-413-p was a potent Wnt/β-catenin agonist but also indicated that Wnt/β-catenin signaling can be induced in ECs with an endogenous level of FZD4 expression. To further confirm the induction of Wnt/β-catenin signaling, expression of the Wnt target gene, *Axin2*, was assessed. *Axin2* mRNA was potently expressed by the SZN-413-p treatment in both ECs (Figs. 2I, 2J). The dose-dependent activity of SZN-413-p was further observed in rabbit retinal microvascular endothelial cells (Supplementary Fig. S2D).

SZN-413-p Induces Tight Junction Proteins in Retinal Vascular Endothelial Cells

Accumulation of lymphoid enhancer binding factor 1 (Lef1) and major facilitator superfamily domain-containing protein 2 (Mfsd2a) has been observed in the BBB vessels with specialized EC tight junctions, which are under Wnt/β-catenin signaling regulation.[25,27,40] mRNA expression of the *LEF1* and *MFSD2A* was also significantly upregulated by SZN-413-p treatment in HRMECs (Fig. 3A). Furthermore, the expression of endothelial tight junction proteins, claudin-5 (CLDN5) and zonula occludens-1 (ZO-1), was upregulated in the retinal vascular ECs after SZN-413-p treatment (Fig. 3B). These results suggest that the bioengineered tetravalent antibody targeting FZD4 and LRP5 is active in vascular ECs and can increase vascular integrity through upregulation of barrier function proteins.

The Novel FZD4 Agonist Inhibits Pathologic Neovascular Tuft Formation and Reduces AV Areas in the Ischemic Retina

In order to develop SZN-413-p into a potential therapeutic candidate, both anti-LRP5 and anti-FZD4

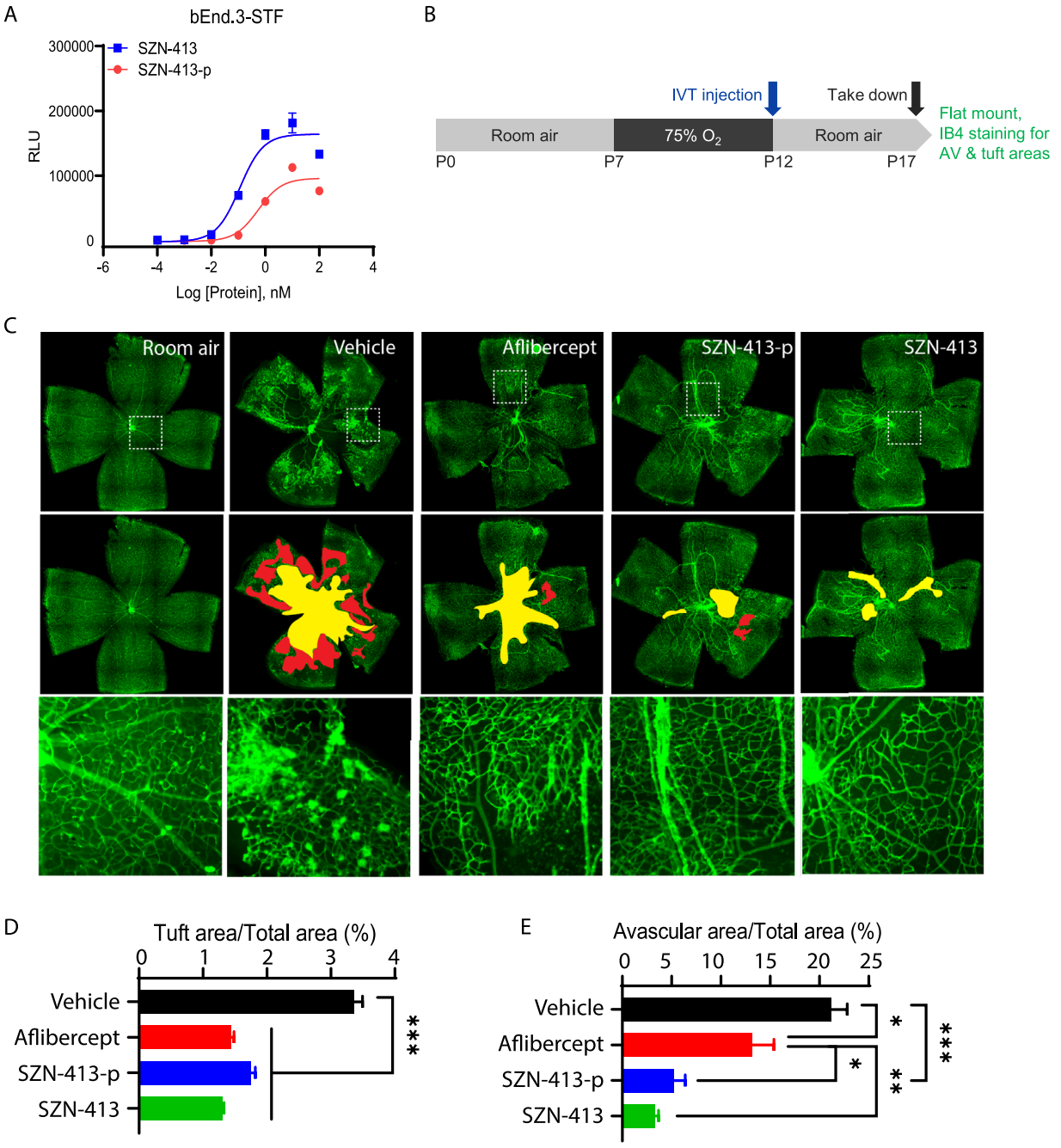

Figure 4. FZD4-specific agonists inhibited retinopathy pathology in OIR mice. (A) Dose-dependent STF activities of SZN-413-p or SZN-413 in bEnd.3 cells. (B) Timeline of the OIR mouse model. Vehicle, SZN-413-p, SZN-413, and aflibercept were administered by intravitreal injection at P12, and all mice were euthanized at P17 for retinal flatmounts. (C) Representative retinal flatmount images. The NV areas are indicated in *red*, and the AV areas are highlighted in *yellow* (*middle panels*). The enlarged areas (*bottom panels*) in the *dotted boxes* (*upper panels*) show the pathologic NV tufts. (D, E) Histograms representing the results of morphometric analysis of retinal flatmounts measuring the area of NV tufts (D) and AV areas (E). Values are mean ± SEM; $*P < 0.05$, $**P < 0.01$, $***P < 0.001$.

domains were humanized, and potential chemical instability sites in complementarity-determining regions were mutagenized to more stable residues. We named the final variant SZN-413. SZN-413 retained its binding specificity to FZD4 (Supplementary Figs. S3A, S3B), with slightly increased affinity (Supplementary Figs. S2B, S3C), and induced Wnt/β-catenin signaling in bEnd.3 cells with and an EC_{50} approximately five to ten times lower than its parental form, SZN-413-p (Fig. 4A).

We next examined how the FZD4 agonists affected retinal vasculature in the OIR mouse model. Mouse

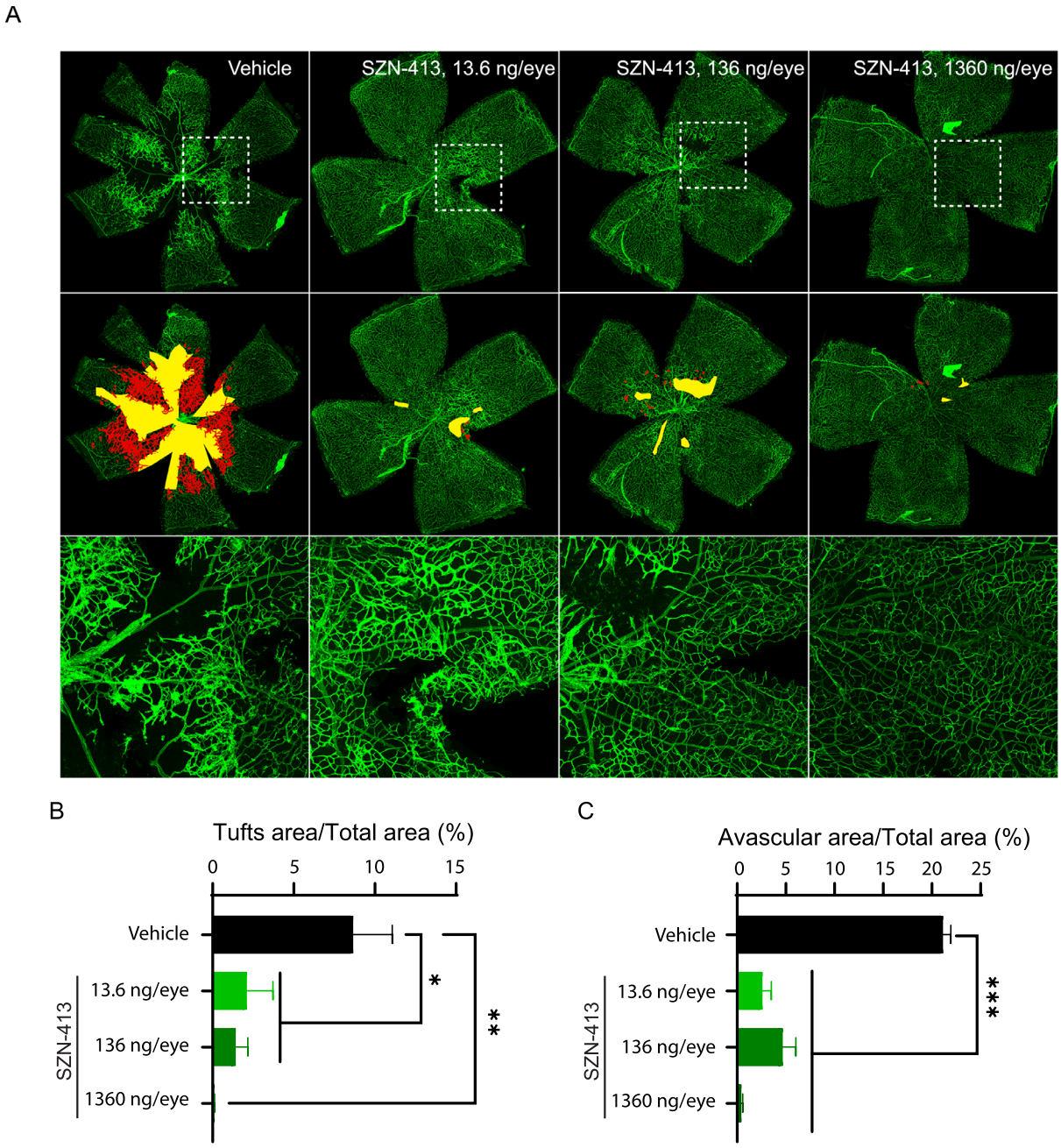

Figure 5. Dose–efficacy relationship for SZN-413 in OIR mice. (A) SZN-413 (13.6 ng/eye, 136 ng/eye, or 1360 ng/eye) or vehicle was administered by intravitreal injection at P12, and all mice were euthanized at P17 for retinal flatmounts. Representative retinal flatmount images are shown. The NV areas are indicated in *red*, and the AV areas are highlighted in *yellow* (*middle panels*). The enlarged areas (*bottom panels*) in the *dotted boxes* (*upper panels*) show the pathologic NV tufts. (B, C) Histograms representing the results of morphometric analysis of retinal flatmounts measuring the area of NV tufts (B) and AV areas (C). Values are mean ± SEM; $^{*}P < 0.05$, $^{**}P < 0.01$, $^{***}P < 0.001$.

pups were moved into 75% oxygen at P7 for 5 days, followed by a return to room air until P17. Mice received intravitreal injections of vehicle, aflibercept, SZN-413-p, or SZN-413 at P12 (Fig. 4B). Compared with negative control (vehicle), both SZN-413-p and SZN-413 significantly reduced the pathologic NV area to an extent comparable to the positive control (aflibercept-treated) group (Figs. 4C, 4D). Surprisingly, the FZD4 agonists also significantly reduced the retinal AV area to a larger degree than the vehicle- or aflibercept-treated groups (Figs. 4C, 4E), suggesting that a FZD4 agonist can induce normal retinal vessel regrowth while suppressing pathologic vessel growth. We further examined the dose–efficacy relationship

of SZN-413 in the OIR model. Mice received intravitreal injections of 13.6 ng, 136 ng, and 1360 ng of SZN-413 or vehicle at P12. All tested doses of SZN-413 showed significant reductions of both pathologic NV and retinal AV areas to a larger degree than the vehicle-treated group (Fig. 5). These results suggest that the novel FZD4 agonist SZN-413 not only potently inhibits pathologic NV tuft formation in retinal ischemic conditions but also potentially promotes proper vessel regeneration to re-perfuse the damaged retina.

SZN-413 Treatment Dramatically Inhibits VEGF-Induced Pathologic Vascular Leakage

We further examined whether our FZD4 agonist could inhibit VEGF-driven retinal leakage. Intravitreal injections of vehicle or four different doses (0.08, 0.4, 2, or 10 µg/eye) of SZN-413 were followed by intravitreal injections of 1 µg of recombinant human $VEGF_{165}$ into Dutch Belted rabbits. Scanning ocular fluorophotometry was used to non-invasively measure fluorescein leakage from retinal vasculature at days 0, 3, and 5

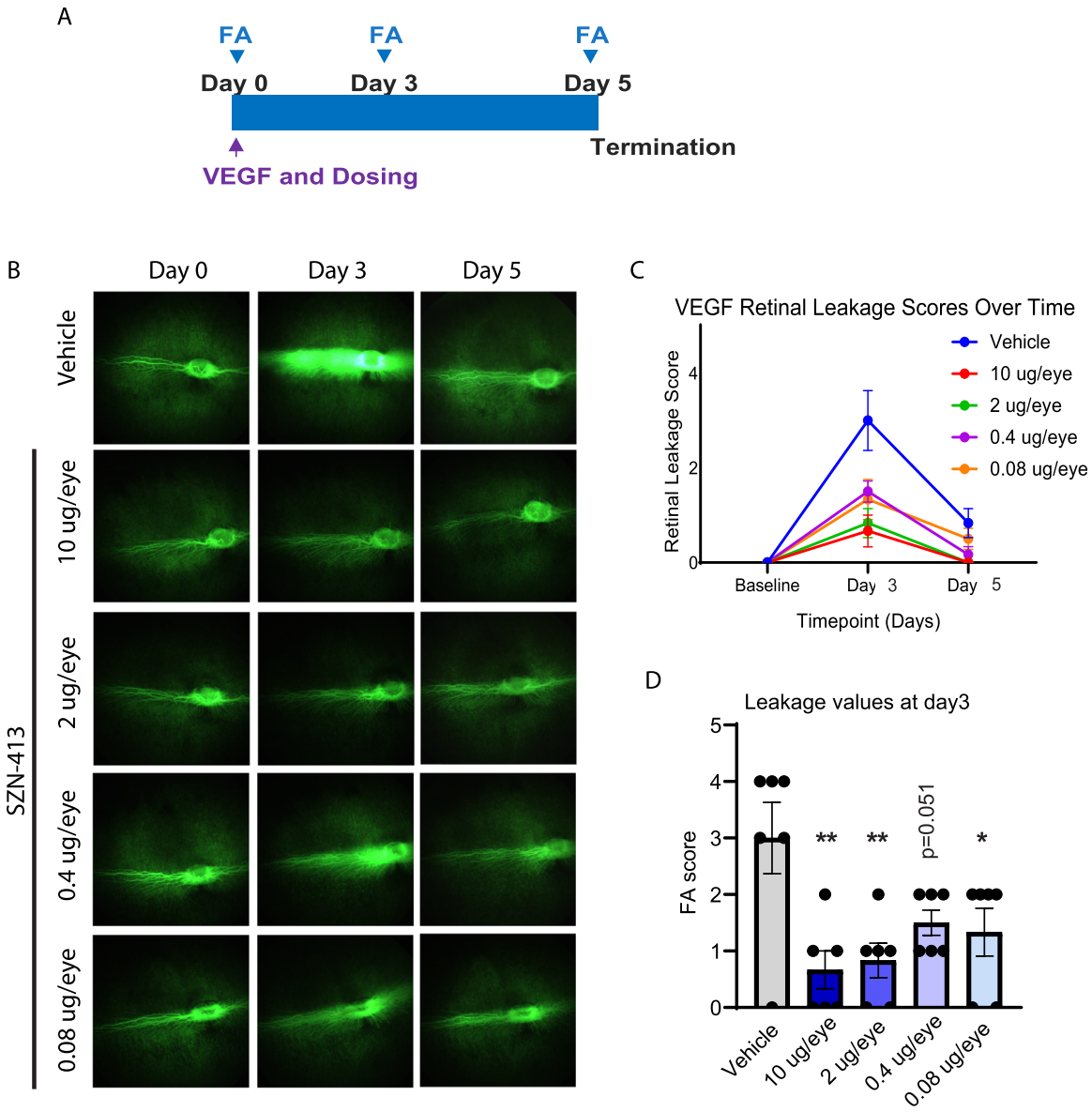

Figure 6. SZN-413 inhibited VEGF-driven retinal vascular leakage. (A) Timeline of the VEGF-induced retinal vascular leakage rabbit model. Vehicle or four dose levels of SZN-413 were administered by intravitreal injection at day 0. Retinal leakage was monitored at days 0, 3, and 5 by FA. (B) Representative FA images from each group of indicated treatments. (C) Trends of retinal leakage score changes in each group. The leak levels peaked on day 3, after which they regressed on day 5 in all groups. (D) Histograms representing the FA scores of each group at day 3. Values are mean ± SEM; *$P < 0.05$, **$P < 0.01$.

(Fig. 6A). The leakage was assessed in a blinded manner, and the collected images were scored for retinal leakage by two trained scorers. Maximal vascular leakage was observed on day 3 after the VEGF intravitreal injection (Figs. 6B, 6C). All doses of SZN-413 successfully inhibited the VEGF-driven retinal vascular leakage, reaching ~80% at the dose of 10 µg/eye compared to the control group (Figs. 6B, 6D). This efficacy was observed in all animals treated with SZN-413 (Supplementary Fig. S4), suggesting that SZN-413 can effectively and directly inhibit retinal vascular leakage in the presence of VEGF. Ocular inflammation and tolerability were assessed with ocular examinations on days 3 and 5 post-injection, and the ocular examination scores for all animals among all groups were generally 0 at both time points measured, indicating that SZN-413 is well tolerated in rabbit eyes (Supplementary Table S1).

Discussion

In the diabetic retina, hyperglycemia-induced microangiopathy results in vascular leakage, causing DME and capillary occlusion, as well as retinal ischemia leading to the overproduction of multiple signaling molecules responsible for the development of pathologic neovascularization and the proliferative stage of diabetic retinopathy.[5,17,41,42] In addition to anti-VEGF therapy, peripheral retinal ischemia can be treated with laser photocoagulation by destroying the ischemic retina leading to peripheral visual field loss and a reduction of total VEGF production in the eye and the drive toward neovascularization.[43] However, there are currently no treatments for diabetic macular ischemia. Laser treatment would not be appropriate, as it could result in central vision loss. Also, the currently approved anti-VEGF treatments for DME and DR reduce vascular leakage and regress pathologic neovascularization but have not been shown to induce reperfusion.[5]

Norrin/FZD4 signaling is indispensable in both proper formation of the retinal vessels during development and for maintaining the barrier function of the retina vessels in adults.[16,17,20,22,26,42] Indeed, our data showed that the FZD4-specific agonist SZN-413 significantly reduced not only pathologic NV tufts but also the damage-induced AV area in an OIR mouse model (Figs. 4, 5), suggesting that SZN-413 may be able to transform pathologic neovascularization into physiological neovascularization, reducing retinal ischemia and the ensuing overproduction of signaling molecules such as VEGF in DR.

In addition, SZN-413 strongly inhibited VEGF-driven retinal vascular leakage in rabbit eyes (Fig. 6). Unlike the current standard-of-care anti-VEGF therapies, our FZD4 agonist acts directly on damaged blood vessels, restoring vascular integrity and physiological neovascularization. The totality of these findings suggests that FZD4 agonism can simultaneously address the retinal non-perfusion and leakage characteristics of DR pathology and may serve as a new therapeutic approach for patients with DR with or without DME. To measure efficacy in future clinical trials, in addition to the accepted endpoints of improvements in visual acuity and reductions in the DRSS, we may want to include optical coherence tomography angiography and ultra-widefield FA to assess the effect of SZN-413 on diabetic macular ischemia.[44]

Recently, a distinct FZD4 agonist, F4L5.13, a tetravalent diabody with a dumbbell-like structure against FZD4 and LRP5, showed comparable maximal STF response to recombinant Norrin.[23] Interestingly, the F4L5.13 did not significantly decrease the AV area in an OIR mouse model study. Although this discrepancy must be further investigated, it may have been caused by differences in potency between the different FZD4 agonists, as SZN-413-p and SZN-413 are more potent than recombinant Norrin (Fig. 2F). Though these different Norrin mimetics were not compared side-by-side nor against the same Norrin preparation, these results may suggest that appropriate molecular format and geometry may be critical to induce Wnt/β-catenin signaling.[28]

This novel mechanism of action of our Norrin mimetic opens new possibilities to treat diabetic and potentially other retinopathies. Furthermore, it is possible that, because SZN-413 regenerates normal retinal vasculature in ischemic areas of the retina, the frequency of anti-VEGF intravitreal injections can be reduced. Moreover, because Norrin/FZD4 signaling is essential for BBB function,[17,24] FZD4 agonism could be also beneficial in circumstances where the BBB is compromised, such as stroke, potentially expanding the indications for SZN-413.

Acknowledgments

The authors thank Hans Clevers, K. Christopher Garcia, Calvin Kuo, Roel Nusse, and other members of our board of directors and scientific advisory group for helpful discussions and suggestions. The authors also thank Geertrui Vanhove for scientific insight and Anna Kido (both with Surrozen) for editorial support. Powered Research, a contract research organization in North Carolina, conducted the unbiased VEGF-induced retinal hemorrhage study. All studies were funded by Surrozen Operating, Inc. A patent

application is pending for the work described in this manuscript.

Disclosure: **H. Nguyen**, Surrozen Operating, Inc. (E, F, I); **H. Chen**, Surrozen Operating, Inc. (E, F, I, P); **M. Vuppalapaty**, Surrozen Operating, Inc. (E, F, I); **E. Whisler**, Surrozen Operating, Inc. (E, F, I); **K.R. Logas**, Surrozen Operating, Inc. (E, F, I); **P. Sampathkumar**, Surrozen Operating, Inc. (E, F, I); **R.B. Fletcher**, Surrozen Operating, Inc. (E, F, I); **A. Sura**, Surrozen Operating, Inc. (E, F, I); **N. Suen**, Surrozen Operating, Inc. (E, F, I); **S. Gupta**, Surrozen Operating, Inc. (E, F, I); **T. Lopez**, Surrozen Operating, Inc. (E, F, I); **J. Ye**, Surrozen Operating, Inc. (E, F, I); **S. Tu**, Surrozen Operating, Inc. (E, F, I, P); **M. Bolaki**, Surrozen Operating, Inc. (E, F, I); **W.-C. Yeh**, Surrozen Operating, Inc. (E, F, I, P, S); **Y. Li**, Surrozen Operating, Inc. (E, F, I, P); **S.-J. Lee**, Surrozen Operating, Inc. (E, F, I, P)

References

1. Cheung N, Mitchell P, Wong TY. Diabetic retinopathy. *Lancet*. 2010;376:124–136.
2. Klein BE. Overview of epidemiologic studies of diabetic retinopathy. *Ophthalmic Epidemiol*. 2007;14:179–183.
3. Moss SE, Klein R, Klein BE. The 14-year incidence of visual loss in a diabetic population. *Ophthalmology*. 1998;105:998–1003.
4. Flaxman SR, Bourne RRA, Resnikoff S, et al. Global causes of blindness and distance vision impairment 1990–2020: a systematic review and meta-analysis. *Lancet Glob Health*. 2017;5:e1221–e1234.
5. Wykoff CC, Yu HJ, Avery RL, Ehlers JP, Tadayoni R, Sadda SR. Retinal non-perfusion in diabetic retinopathy. *Eye (Lond)*. 2022;36:249–256.
6. Abraham JR, Wykoff CC, Arepalli S, et al. Exploring the angiographic-biologic phenotype in the IMAGINE study: quantitative UWFA and cytokine expression [published online ahead of print June 7, 2021]. *Br J Ophthalmol,* https://doi.org/10.1136/bjophthalmol-2020-318726.
7. Simo R, Hernandez C. Intravitreous anti-VEGF for diabetic retinopathy: hopes and fears for a new therapeutic strategy. *Diabetologia*. 2008;51:1574–1580.
8. Zampros I, Praidou A, Brazitikos P, Ekonomidis P, Androudi S. Antivascular endothelial growth factor agents for neovascular age-related macular degeneration. *J Ophthalmol*. 2012;2012:319728.
9. Miller JW, Le Couter J, Strauss EC, Ferrara N. Vascular endothelial growth factor A in intraocular vascular disease. *Ophthalmology*. 2013;120:106–114.
10. Rodrigues EB, Farah ME, Maia M, et al. Therapeutic monoclonal antibodies in ophthalmology. *Prog Retin Eye Res*. 2009;28:117–144.
11. Brown DM, Wykoff CC, Boyer D, et al. Evaluation of intravitreal aflibercept for the treatment of severe nonproliferative diabetic retinopathy: results from the PANORAMA randomized clinical trial. *JAMA Ophthalmol*. 2021;139:946–955.
12. Ip MS, Domalpally A, Hopkins JJ, Wong P, Ehrlich JS. Long-term effects of ranibizumab on diabetic retinopathy severity and progression. *Arch Ophthalmol*. 2012;130:1145–1152.
13. Ip MS, Domalpally A, Sun JK, Ehrlich JS. Long-term effects of therapy with ranibizumab on diabetic retinopathy severity and baseline risk factors for worsening retinopathy. *Ophthalmology*. 2015;122:367–374.
14. Maturi RK, Glassman AR, Josic K, et al. Effect of intravitreous anti-vascular endothelial growth factor vs sham treatment for prevention of vision-threatening complications of diabetic retinopathy: the Protocol W randomized clinical trial. *JAMA Ophthalmol*. 2021;139:701–712.
15. Junge HJ, Yang S, Burton JB, et al. TSPAN12 regulates retinal vascular development by promoting Norrin- but not Wnt-induced FZD4/beta-catenin signaling. *Cell*. 2009;139:299–311.
16. Paes KT, Wang E, Henze K, et al. Frizzled 4 is required for retinal angiogenesis and maintenance of the blood–retina barrier. *Invest Ophthalmol Vis Sci*. 2011;52:6452–6461.
17. Wang Y, Rattner A, Zhou Y, Williams J, Smallwood PM, Nathans J. Norrin/Frizzled4 signaling in retinal vascular development and blood brain barrier plasticity. *Cell*. 2012;151:1332–1344.
18. Ye X, Wang Y, Cahill H, et al. Norrin, frizzled-4, and Lrp5 signaling in endothelial cells controls a genetic program for retinal vascularization. *Cell*. 2009;139:285–298.
19. Gariano RF, Gardner TW. Retinal angiogenesis in development and disease. *Nature*. 2005;438:960–966.
20. Kondo H, Kusaka S, Yoshinaga A, Uchio E, Tawara A, Tahira T. Genetic variants of *FZD4* and *LRP5* genes in patients with advanced retinopathy of prematurity. *Mol Vis*. 2013;19:476–485.
21. Yang H, Li S, Xiao X, Wang P, Guo X, Zhang Q. Identification of *FZD4* and *LRP5* mutations in 11 of 49 families with familial exudative vitreoretinopathy. *Mol Vis*. 2012;18:2438–2446.

22. Ye X, Wang Y, Nathans J. The Norrin/Frizzled4 signaling pathway in retinal vascular development and disease. *Trends Mol Med*. 2010;16:417–425.
23. Chidiac R, Abedin M, Macleod G, et al. A Norrin/Wnt surrogate antibody stimulates endothelial cell barrier function and rescues retinopathy. *EMBO Mol Med*. 2021;13:e13977.
24. Wang Y, Cho C, Williams J, et al. Interplay of the Norrin and Wnt7a/Wnt7b signaling systems in blood–brain barrier and blood–retina barrier development and maintenance. *Proc Natl Acad Sci USA*. 2018;115:E11827–E11836.
25. Wang Z, Liu CH, Huang S, et al. Wnt signaling activates MFSD2A to suppress vascular endothelial transcytosis and maintain blood–retinal barrier. *Sci Adv*. 2020;6:eaba7457.
26. Diaz-Coranguez M, Lin CM, Liebner S, Antonetti DA. Norrin restores blood–retinal barrier properties after vascular endothelial growth factor-induced permeability. *J Biol Chem*. 2020;295:4647–4660.
27. Wang Y, Sabbagh MF, Gu X, Rattner A, Williams J, Nathans J. Beta-catenin signaling regulates barrier-specific gene expression in circumventricular organ and ocular vasculatures. *eLife*. 2019;8:e43257.
28. Chen H, Lu C, Ouyang B, et al. Development of potent, selective surrogate WNT molecules and their application in defining frizzled requirements. *Cell Chem Biol*. 2020;27:598–609.e4.
29. Janda CY, Dang LT, You C, et al. Surrogate Wnt agonists that phenocopy canonical Wnt/β-catenin signalling. *Nature*. 2017;545:234–237.
30. Zhang Z, Broderick C, Nishimoto M, et al. Tissue-targeted R-spondin mimetics for liver regeneration. *Sci Rep*. 2020;10:13951.
31. Macosko EZ, Basu A, Satija R, et al. Highly parallel genome-wide expression profiling of individual cells using nanoliter droplets. *Cell*. 2015;161:1202–1214.
32. Cole MB, Risso D, Wagner A, et al. Performance assessment and selection of normalization procedures for single-cell RNA-seq. *Cell Syst*. 2019;8:315–328.e8.
33. Lun AT, Bach K, Marioni JC. Pooling across cells to normalize single-cell RNA sequencing data with many zero counts. *Genome Biol*. 2016;17:75.
34. Menon M, Mohammadi S, Davila-Velderrain J, et al. Single-cell transcriptomic atlas of the human retina identifies cell types associated with age-related macular degeneration. *Nat Commun*. 2019;10:4902.
35. Smith LE, Wesolowski E, McLellan A, et al. Oxygen-induced retinopathy in the mouse. *Invest Ophthalmol Vis Sci*. 1994;35:101–111.
36. Hackett RBM, T. O. Ophthalmic toxicology and assessing ocular irritation. In: Marzulli FN, Maibach HI, eds., *Dermatotoxicology.* Washington, DC: Hemisphere Publishing; 1996:749–815.
37. Xia CH, Liu H, Cheung D, et al. A model for familial exudative vitreoretinopathy caused by LPR5 mutations. *Hum Mol Genet*. 2008;17:1605–1612.
38. Xia CH, Yablonka-Reuveni Z, Gong X. LRP5 is required for vascular development in deeper layers of the retina. *PLoS One*. 2010;5:e11676.
39. Fowler TW, Mitchell TL, Janda CY, et al. Development of selective bispecific Wnt mimetics for bone loss and repair. *Nat Commun*. 2021;12:3247.
40. Ben-Zvi A, Lacoste B, Kur E, et al. Mfsd2a is critical for the formation and function of the blood–brain barrier. *Nature*. 2014;509:507–511.
41. Drenser KA. Wnt signaling pathway in retinal vascularization. *Eye Brain*. 2016;8:141–146.
42. Robitaille J, MacDonald ML, Kaykas A, et al. Mutant frizzled-4 disrupts retinal angiogenesis in familial exudative vitreoretinopathy. *Nat Genet*. 2002;32:326–330.
43. Evans JR, Michelessi M, Virgili G. Laser photocoagulation for proliferative diabetic retinopathy. *Cochrane Database Syst Rev*. 2014;2014(11):CD011234.
44. Cheung CMG, Pearce E, Fenner B, Sen P, Chong V, Sivaprasad S. Looking ahead: visual and anatomical endpoints in future trials of diabetic macular ischemia. *Ophthalmologica*. 2021;244:451–464.